

ATMOSPHERIC ABSORPTION MEASUREMENT BY FOURIER TRANSFORM DOAS

A CONTRIBUTION TO THE EUROTRAC SUBPROJECT TOPAS

Annual Report 1991

- R. COLIN and M. CARLEER
Laboratoire de Chimie Physique Moléculaire (ULB)
Université Libre de Bruxelles, CP 160
50, av. F.D. Roosevelt
B-1050 Brussels
Belgium
- P.C. SIMON and A.-C. VANDAELE
Institut d'Aéronomie Spatiale de Belgique (IASB)
3, av. Circulaire
B-1180 Brussels
Belgium
- P. DUFOUR and C. FAYT
Laboratoire d'Informatique (UMH)
Université de Mons-Hainaut
15 av. Maistriau
B-7000 Mons
Belgium

Contents

I Introduction

II Use of a Fourier Spectrometer for Tropospheric Measurements in the Optical Region

II.1 Instrumental set up

II.2 Measurements of Absorption Cross Sections of SO₂ and NO₂

II.3 Data Analysis and Results

II.4 Discussion

II.4.1 Comparison with Grating Instruments

II.4.2 Comparison with Chemical Measurements : the Case of NO

II.5 Conclusions and projects

III Software Development for a Grating Spectrometer

III.1 Description of the Instrument

III.2 Interfacing with the Instrument

III.2.1 Hardware Description

III.2.2 Software Description

III.2.3 Instrument Automation

IV General Conclusions and Future Works

I Introduction

The objective of the EUROTRAC-TOPAS subproject is to develop high performance instruments based on differential optical absorption spectroscopy (DOAS) in order to measure minor constituents of the troposphere. In this framework, the Belgian groups have, in the course of 1991, made the following contributions :

- A study of the use of Fourier Transform Spectroscopy (ULB-IASB)
- Development of software for a grating spectrometer (UMH-IASB)

DOAS can provide a simultaneous measurement of the concentration of several atmospheric species. These concentrations of the different molecules are deduced using the Beer-Lambert law :

$$I(\lambda) = I_o(\lambda)e^{-\sum_i^N n_i\sigma_i(\lambda)d} \quad (1)$$

where $I(\lambda)$ is the measured intensity

$I_o(\lambda)$ is the intensity of the lamp without any absorption

n_i is the concentration of the i^{th} species

$\sigma_i(\lambda)$ is the cross section of the i^{th} species

d is the optical path

$I_o(\lambda)$ is not a measurable quantity when atmospheric absorption is concerned; therefore relation 1 has to be rewritten as :

$$I(\lambda) = I'_o(\lambda)e^{-\sum_i^N n_i\Delta\sigma_i(\lambda)d} \quad (2)$$

where $\Delta\sigma_i(\lambda)$ is the differential cross section of the i^{th} species and I'_o is the measured intensity from which all absorption structures have been removed. Several mathematical methods can be used to derive I'_o from experimental spectra. Some of these will be discussed and compared in the present report.

Differential cross sections $\Delta\sigma(\lambda)$ are derived from the absolute cross sections. It is important that they be derived with the same technique than the one used to derive I'_o from I.

The performances of the DOAS technique combined with a Fourier Transform Spectrometer (FTS) will be described in section II, with results concerning new absorption cross sections measurements made with the FTS, and concerning tropospheric measurements of SO_2 , NO_2 and O_3 . Discussion of biases introduced by the different methods will be presented.

Once $\Delta\sigma_i(\lambda)$ and I'_o are known, a least squares procedure can be applied on the optical thickness, in order to determine the concentrations of the absorbing constituents.

An improved software for the operation of a grating spectrometer will be discussed in section III.

Finally the future works will be presented in the last section.

II Use of a Fourier Transform Spectrometer for tropospheric measurements in the optical region

II.1 Instrumental set up

The experimental arrangement is shown in figure 1a. The light source consists either of a 800 Watt "ozone free" Xenon lamp or of a Tungsten filament, depending on the spectral range studied. The Xenon lamp, used for the UV/Visible region is enclosed in a envelope preventing transmission of ultraviolet light which could possibly create ozone within the lamp housing, thereby affecting the quality of the ozone measurements. The Tungsten filament is used when working in the visible range.

The light is collimated onto a 30 cm Cassegrain-type telescope, which projects the beam onto a slightly parabolic mirror, situated 394 m away. This mirror sends the beam back into a second 30 cm Cassegrain telescope, which collimates the light onto the entrance aperture of a BRUKER IFS120HR Fourier transform Spectrometer. The detector is a solar blind UV- or a Si-diode depending on the spectral range.

Considering the fact that the absorption features of the molecules to be detected are broad (O_3) or even diffuse (SO_2), no advantage is gained by operating at the best possible resolution offered by the instrument. Spectra have been recorded at 2, 4, 8 and 16 cm^{-1} and it has been decided that a resolution of 16 cm^{-1} (0.15 nm at 300 nm) was a good compromise between resolution and signal to noise ratio.

Table 1 summarizes the characteristics of the experimental set-up when working in the UV/Visible region or the Visible region.

Table 1 : Characteristics of the experimental set-up

	Spectral region (cm^{-1})	Lamp	Beam-splitter	Detector	Molecules detected	Other possible molecules
UV/Visible	26000-38000 (260-380 nm)	Xenon	Suprasil	Solar blind Diode	SO_2 , NO_2 , O_3 , O_2	H_2CO , CS_2
Visible	14000-30000 (330-700 nm)	Tungsten	Infrasil	Si Diode	NO_2 , H_2O NO_3	

II.2 Measurements of absorption cross sections of SO_2 and NO_2

Absorption cross sections of SO_2 and NO_2 have been measured with the FTS in the UV/Visible spectral range (26000-38000 cm^{-1}) at different resolutions (2, 4, 8 and 16 cm^{-1}) and at room temperature.

The measurements have been performed with the experimental set-up shown in figure 1b. The purpose for measuring a new set of cross sections was to record them in the same experimental conditions and on the same instrument used for recording the atmospheric spectra, in order to eliminate any instrumental effects in the fitting procedure between measured and calculated optical thickness.

The gas, either SO₂ or NO₂, is introduced in small quantities in a 20 cm long absorption cell; air is added to obtain a total pressure of 1 atmosphere. The partial pressure of the analysed gas is measured with a Baratron gauge and the temperature is monitored with a conventional sensor.

The cross sections of SO₂ and NO₂ are obtained using Beer-Lambert law

$$\sigma(\lambda) = \frac{1}{nd} \ln \frac{I_0(\lambda)}{I(\lambda)} \quad (3)$$

where n denotes the concentration of the gas (SO₂ or NO₂), d the length of the cell, I is the measured intensity of the filled cell and I₀ the measured intensity when the cell is empty. When possible, two blanks have been taken, one before and one after the measurement of I, so that I₀ is taken as the mean value of those two blanks. Table 2 gives the various conditions of the SO₂ and NO₂ cross sections measurements.

Table 2 : Conditions for the SO₂ and NO₂ cross sections measurements

	Pressure (mb)	Temperature (°C)	Resolution (cm ⁻¹)	Number of scans
NO ₂	5.00	19.0	2	2000
	5.00	21.0	4	2000
	5.00	21.0	8	2000
	5.00	20.0	16	2000
SO ₂	0.5	20.5	2	2000
	0.5	20.5	4	2000
	0.5	21.5	8	2000
	0.5	20.0	16	2000

To determine the concentration of NO₂, the N₂O₄ ⇌ 2 NO₂ equilibrium with its dimer must be considered. The partial pressure of both constituents are calculated using the value of the equilibrium constant taken from Stull and al.[1]. The spectral features of N₂O₄ were not removed from the experimental spectra, as concentration of N₂O₄ were always small. It is to be noticed that this should not influence the values of the differential cross sections of NO₂ as N₂O₄ only presents a continuous absorption spectrum[2][3].

Differential cross sections are obtained from our measurements using Fourier transform filtering. This technique will be fully detailed in the following chapter. Absolute and differential cross sections of SO₂ and NO₂ at the resolution of 16 cm⁻¹ are plotted in figures 2,3,4 and 5.

To evaluate the error limits of the cross sections measurements, several points were taken into account : errors on the pressure and temperature measurements, uncertainty on the absorption path length, presence of impurities in the samples and error on the absorbance. It should be mentioned that, between blank and absorption measurements, the cell is not removed from the spectrometer, thus no error due to the changing of the geometry of the set-up is introduced. The error budget is given in Table 3. According to these, the accuracy on the cross sections of SO₂ is of the order of ±2 % and of the order of ±5% in the case of NO₂.

Table 3 : Estimation of errors limits on cross sections measurements

	NO ₂ %	SO ₂ %
Optical path (19.9cm±0.1 cm)	0.5	0.5
Pressure (0.1% in the range 10mb)	0.1	0.1
Temperature (293K±0.5K)	0.2	0.2
Impurities in the sample	4	0.02
Absorbance ln(I ₀ /I) τ=1	2	2
Total rms	±5%	±2%

The absolute and differential cross sections measured in this work have been compared to data from the literature. The results concerning NO₂ were compared to the data of Schneider et al.[4]. The absolute cross sections are in good agreement in the wavenumber range 30830 - 33780 cm⁻¹ (better than 10%), however discrepancies appear in the ranges 26300 - 30830 cm⁻¹ and 33780 - 42300 cm⁻¹ (more than 10%). In the latter region this could be due to the fact that the signal to noise ratio of the spectrum of the present work is very low, due to the end of the sensitivity of the detector in this region. It appears that the cross sections measured by Schneider et al.[4] could present some anomalies regarding the wavelength calibration. This could explain the discrepancies observed in the wavenumber region 26300-30830 cm⁻¹. The comparison between the cross sections of SO₂ of this work and of Thomsen[5], shows that the data are in good agreement (better than 5%).

Ozone cross sections were not measured but were taken from Daumont et al.[6].

II.3 Data analysis and results

As already explained in the introduction, the DOAS technique is based on the determination of a "reference spectrum" I₀' derived mathematically from the experimental spectrum. Numerous methods for determining I₀' exist. The three following have been used in this work.

1. Fourier transform filtering consists in removing the lower frequencies portion of the power spectrum of the experimental data. This method is based on the fact that the general curve of an experimental spectrum (fig 6.a) corresponds to a slow variation of intensity with wavenumber. In the Fourier domain (fig 6.b), function of the inverse of wavenumber (here called frequency space by analogy with classical Fourier analysis) this slow variation is associated to the lower frequencies of the power spectrum. The power spectrum of the experimental data h(ν) is obtained using its definition :

$$P(f) = 2 | H(f) |^2 \quad (4)$$

where H(f) represents the Fourier transform of the function h(ν). This definition is only valid when the function h(ν) is real, as it is in present case.

Filtering is accomplished using a low pass filter (represented by a dashed line in

figure 6.b). The limits of this filter have been chosen so that all the fine structures are removed from the spectra. Inverse Fourier transform of the low frequencies of the power spectrum provides the function I'_0 defined earlier and a differential spectrum can be obtained (fig 6.c).

The Fast Fourier Transform (FFT) algorithm was chosen to calculate the Fourier transform of the spectra. It is to be remembered that this algorithm imposes some conditions on the spectrum to be processed :

- (a) the number of points must be a power of 2
- (b) any time a fast variation in the values in the spectrum occurs, FFT produces artifact functions of the form $\frac{\sin x}{x}$. In order to avoid this problem at the boundaries, the spectrum is driven smoothly to zero at the extremities, by application of a mask.

The latter point implies another problem encountered with Fourier transform filtering. The Xenon lamp, for example, emits a nearly continuous spectrum, but some intense emission peaks are present. As figure 6.a shows, these peaks are not negligible in amplitude compared to the molecular absorption structures to be detected. Moreover, they are very narrow and they introduce $\frac{\sin x}{x}$ functions which greatly distort the differential spectrum. This effect can clearly be seen on figure 7, where the differential spectrum of the Xenon lamp taken without passing through the telescopes is represented. The smaller the atmospheric absorption features, the greater is this effect.

2. To avoid this phenomenon another method has been developed, which, before Fourier filtering, consists in the removal of the emission peaks of the lamp from the experimental spectrum. Such doing, the influence of the distortion is reduced.
3. Another method, based on polynomial interpolation, was used to determine the function I'_0 from the experimental spectra. In this method, the experimental spectrum is divided into three regions, delimited by either an extremity of the spectrum or an emission peak of the Xenon lamp, in such a way as to totally remove these peaks from the analysed regions. A least squares procedure is applied to each of these regions in order to determine the best polynome representing the general shape of the curve. The degree of this polynome is either 4 or 5. This polynome is then used as the function I'_0 .

It is important to note that, whatever the chosen method is, it is necessary to process the cross sections of the absorbing molecules in exactly the same way, as this will avoid additional distortion between the experimental differential spectrum and the cross sections. It is, however, never fully possible to work in exactly the same conditions. For example, in the absorption spectrum used to measure cross sections, the concentration of the absorber can be such that any influence of the emission peaks of the lamp is canceled out. It could therefore be valuable to record absorption spectra of the concerned molecules at different concentrations, so that the evolution of the "base line" can be taken into account.

The three methods described above have been compared. The technique used to derive the concentrations was a least squares procedure in all three cases. Table 4 shows the concentrations of SO_2 , NO_2 and O_3 , obtained for different spectra. The relative

and absolute errors on these concentrations are given. As can be seen, there is a great discrepancy in the concentration values found with the different methods.

Table 4 : Comparison of the three methods

atmos. spectrum	molecule	Method 1			Method 2			Method 3		
		n (ppb)	ϵ_{abs} (ppb)	ϵ_{rel} (%)	n (ppb)	ϵ_{abs} (ppb)	ϵ_{rel} (%)	n (ppb)	ϵ_{abs} (ppb)	ϵ_{rel} (%)
27/8/91 10 ^h LT	SO ₂	19.0	0.1	0.5	19.0	0.1	0.5	16.5	0.2	1.2
	O ₃	8	3	38	18	3	17	36	1	3
	NO ₂	78	2	3	85	2	2	88	3	3
27/8/91 11 ^h LT	SO ₂	10.2	0.1	1.0	10.1	0.1	1.0	8.9	0.2	2.3
	O ₃	21	3	14	31	2	7	28	1	4
	NO ₂	38	2	5	45	2	4	48	3	6
27/8/91 12 ^h LT	SO ₂	5.5	0.1	1.8	5.4	0.1	1.9	4.7	0.1	2.1
	O ₃	35	3	9	45	2	4	33	1	3
	NO ₂	26	2	8	34	2	6	37	3	8
27/8/91 13 ^h LT	SO ₂	4.0	0.1	2.5	4.0	0.1	2.5	3.6	0.2	5.6
	O ₃	49	3	6	59	2	3	34	2	6
	NO ₂	11	1	9	18	2	11	19	3	16
27/8/91 14 ^h LT	SO ₂	4.9	0.1	2.0	4.9	0.1	2.0	4.4	0.2	4.6
	O ₃	53	2	4	63	2	3	30	2	7
	NO ₂	20	1	5	26	2	8	28	3	11

SO₂ concentration is relatively constant, due to the fact that the signal to noise ratio for SO₂ is always large. Methods 1 and 2 give very comparable results. Results concerning NO₂ and O₃ are less consistent; variations of a factor 2 or 3 are observed. As cross sections are identical for the three methods, this can only be attributed in the derivation of I₀'. Another problem in determining O₃ concentration is the elimination of the absorption structures of O₂.

As a typical example, figure 8 shows the experimental and calculated spectra obtained with the three methods for the first spectrum of table 4.

Concentration evolutions of SO₂, NO₂ and O₃ for the days May 22, 1991, July 23, 1991 and September 24, 1991 are presented on figure 9. The correlation between NO₂ and O₃ concentrations can clearly be seen. In figure 10, the day concentration of NO₂ is plotted against the day concentration of O₃ for the two days May 23, 1991 and July 23, 1991. The correlation coefficients are respectively 0.97 and 0.98, indicating a strong chemical relation between the two species. Moreover the observed diurnal variation of O₃ suggests that O₃ concentration is mainly determined by photochemical processes.

II.4 Discussion

II.4.1 Comparison with grating instruments

The Fourier Transform Spectrometer has the following advantages against conventional grating spectrometers :

1. The spectral range analysed in one single experiment is larger, 26000-38000 cm^{-1} (260-380 nm) and 14000-30000 cm^{-1} (330-700 nm) when working respectively in the UV and Visible spectral regions.
2. The entrance aperture is a circular hole of large dimension (diameter = 4 mm), allowing more light to enter the spectrometer. This results in a better signal to noise ratio, and thereby provides smaller detection limits.
3. The instrument is calibrated in wavenumber by the use of the Helium-Neon laser interferometer measuring the displacement of the moving mirror with great accuracy.
4. The resolution in the UV/Visible region is essentially limited by the optics quality of the mirrors and beamsplitter, leading to a maximum resolution of the order of 10^{-2} cm^{-1} .

One aim of this research project is to validate the use of Fourier Transform Spectroscopy in the case of atmospheric studies.

The detection limits obtained with the present set up are compared to values obtained with grating instruments in Table 5. Signal to noise ratios for the different molecules are reported. These values are relative to a UV/Visible spectrum recorded in the following conditions :

recorded spectral range = 0-50000 cm^{-1}
analysed spectral range = 26000-38000 cm^{-1}
resolution = 16 cm^{-1}
dispersion = 7.7 cm^{-1}
number of scans = 2000
information stored during the forward and backward
movements of the mirror
time of experiment = 45 min
file size = 27 K

It should be mentioned that the values concerning the grating instruments have been corrected in order to correspond to an optical path of 788 m. It should also be noticed that the instrumentation used by Pommereau et al.[7] have been improved and should now give better detection limits. The high value of the detection limit of the NO_2 is due to the fact that the signal to noise ratio is very low in the UV range used up to now by the FTS. The future measurements will be made in the Visible region, where the detection limit should be lesser.

Table 5 : Detection limits

	$\bar{\nu}$	S/N	Detection Limit			
	(cm^{-1})		(ppb)			
	(1)	(1)	(1)	(2)	(3)	(4)
SO ₂	33340	3200	0.1	3.5	0.09	-
NO ₂	28710	500	5.8	1.7	0.5 ⁺	6.4
O ₃	35305	1700	1.6	1.0	7.4*	133*

(1) This work

(2) Pommereau et al.[7]

(3) Platt et al.[8]

(4) Plane et al.[9]

* at 328 nm (30488 cm^{-1})

+ at 354 nm, 357 nm, 365 nm (28249 cm^{-1} , 28011 cm^{-1} , 27397 cm^{-1})

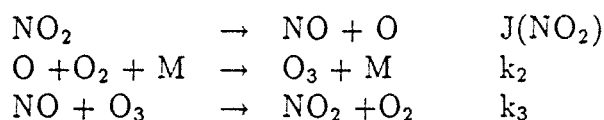
II.1.2 Comparison with chemical measurements : the case of NO

The concentration profiles of O₃ and NO₂ suggest that these two species are related by a strong chemical relation and a photochemical model, considering a steady state for O₃ and atomic oxygen and based upon the Leighton reactions scheme (see Table 6), has been applied. If O₃ is truly in a steady state, then equation 5 holds.

$$\frac{[NO][O_3]}{[NO_2]} = \frac{J(NO_2)}{k_3} \quad (5)$$

where $k_3[\text{cm}^3/\text{molec sec}] = 2.0 \cdot 10^{-12} \exp(-\frac{1400}{T})$ [10] and the photodissociation rate $J(\text{NO}_2)$ is calculated using the empirical relation given by Parrish et al. [11]

Table 6 : Leighton reactions scheme



Using relation 5, concentrations of NO have been derived. The calculated NO concentrations are plotted in figures 11 for February 19, 1991. On the same plot are represented the NO concentration values measured by the Institute for Hygiene and Epidemiology (Brussels). This station is located at Uccle, 3 km from the campus of the ULB and uses a chemical technique to measure NO. The agreement between both sets of values which use quite different techniques, is most satisfactory. The Institute for Hygiene and Epidemiology also performs chemical measurements of SO₂, NO₂ and O₃ and future analysis will be made with these values, leading to the comparison of the two sets of data.

II.5 Conclusions and projects

The system which has been described, has been in operation since October 1990. Since more than one year, measurements have been made once a month over a period of time of 24 hours or more. It is therefore possible to deduce from these data diurnal evolutions of the measured constituents, but seasonal or long term variations are not yet available.

In the future, measurements of cross sections of CS₂, SO₂ and NO₂ at various concentrations and at different temperature conditions will be undertaken in order to examine the problems related to the difficulty in determining the intensity base line.

Another future development is the extension of the measurements to the Visible region. A few spectra have already been recorded and analysed in the region between 14000 and 30000 cm⁻¹. Data analysis is in progress in order to determine concentrations of NO₂, H₂O and NO₃.

III Software developments for a grating spectrograph

III.1 Description of the instrument

A grating spectrograph with a photodiode array as detector has been defined and mounted in order to be able to perform tropospheric absorption measurements using either the same optical long path defined for the Fourier transform spectrograph described in section A or the scattered zenith sunlight which gives the total column abundances of atmospheric species at sunrise and sunset. Absorption measurements using the direct sunlight could also be made provided cloudless sky conditions are met.

The spectrograph used for this project is a 1/8 m crossed Czerny-Turner from ORIEL (type Multispec) with a F number of 3.7. This instrument has a flat focal field adequate for use with photodiode arrays (PDA) up to 25 mm long. Several entrance slits from 25 to 200 μ width are available. Different gratings can be selected according to the required spectral resolution and the wavelength range of interest. The resolution for a PDA spectrograph is defined over two pixels of the detector. Typically, for this spectrograph, a resolution of 0.4 nm can be reached with a grating of 1200 grooves/mm, an entrance slit of 25 μ m and a 1024 elements PDA. In that case, the wavelength range is of the order of 200 nm between 180 nm and 1300 nm, the used interval depending on the blaze angle of the grating. The combination of an entrance slit of 100 μ m with a grating with 600 grooves/mm and a 1024 pixel PDA provides a measured Full Width at Half Maximum (FWHM) of 1.2 nm between 300 and 600 nm. The spectral window extends from 270 to 600 nm. In that case, the sampling defined by the size of the pixel (25 μ m) and the spatial resolution corresponding to the FWHM is 4. The detector is a Reticon PDA of 1024 pixels which can be cooled down to -50°C by the means of a two stages Peltier in order to reduce the dark current. Such a low temperature can be only reached by running methanol at -5°C in a cooling loop connected to an external minicyostat. The other characteristics are summarized in Table 7. The readout electronics has been made by Princeton Instrument Inc. (PI) and provides a dynamic range of 16 bits. The detector assembly is integrated in a vacuum tight container evacuated by a small pump to avoid water vapor freezing on the detector, at low temperature. The grating position is controlled by a stepping motor having an angular resolution of 16 arc sec by step. Filters can be placed in front of the entrance slit in order to exclude second order overlap. The filter wheel has a closed position used to measure the dark count corresponding to the measurement integration time.

Table 7 : Technical specifications of the PDA detector

Number of pixels	1024 pixels
Pixel dimensions	25 μ m x 2.5 mm
Dynamic range	16 bits
Thermoelectric cooling	$T_D \geq -50^\circ$
Quantum efficiency at	
700 nm	$\sim 70^\circ$
300 nm	$\sim 40^\circ$
Readout noise	1 count rms
Sensitivity	1 count = 1300 e ⁻
Dark charge	10 counts/pixels/sec (at - 35 $^\circ$ C)
Leakage current	3 counts/pixels/sec (at - 50 $^\circ$ C)
Well depth	$\neq 7.5 \cdot 10^7 e^-$

III.2 Interfacing with the instrument

III.2.1 Hardware description

Interfacing with the instrument has been achieved with the hardware defined in figure 12. The system includes a compatible IBM 386 AT computer, the ST-1000 detector controller and the spectrograph with a self-scanning photodiode array of 1024 pixels. The oscilloscope is optional. The detector controller (ST-1000) provides power, thermostating and timing signals to the detector head, coordinates data gathering with the experiment, sets exposure time, digitizes and averages data and transmits it to the computer. For a rapid DMA (Direct Memory Access) transfer, the ST-1000 has free access to the AT's 16 bits bus providing a large dynamic range from 0 to 65536 counts. The data bus is used bidirectionally by the computer to send control information bytes to the ST-1000 and to receive raw data back.

III.2.2 Software description

OSMA (Optical Spectrometric Multichannel Analyzer) is the AT software package provided by Princeton Instrument, Inc., with the ST-1000 to control the detector and to perform the data acquisition[12]. The main programme appears to the user as an interactive master menu with options easy to select with cursor or mouse. This menu also uses pulled down menus and queries so that the user can select other options and enter values to prepare the system to take data by defining all the necessary system operation procedures and experimental parameters. In addition to the interface

implemented with the master menu, the software allows realtime viewing of data as it is collected or replaying stored or modified data. It is possible to obtain multiple graphs in a window in order to display simultaneously realtime data and previously stored data and to zoom on certain features of a spectrum while displaying a time history of another spectrum. All the ST-1000 softwares are written in C and 8086 assembler utilizing Lattice C Compiler and Microsoft Macro Assembler.

III.2.3 Instrument Automation

Even though the OSMA software package constituted a very good tool for the user to define all the parameters of an experiment and to manipulate the data provided by the detector, the instrument could not be automated with such a software for the following reasons :

- successive spectra could not be detected with different exposure times and different numbers of scans without interrupting the current experiment;
- the programming of a stepping motor could not be integrated into the OSMA software for the control of a filter wheel in front of the spectrometer slit and to be moved at one of the three positions :
 - open for raw data acquisition;
 - close for dark current acquisition;
 - filter for filtered spectra acquisition;
- the already prohibitive size of OSMA did not allow programming of large sequences of experiments with macro instructions.

Consequently, a new software based on OSMA has been written in order to make possible the instrument automation. The main objectives were to take successive spectra with the filter wheel at different positions and with exposure times and numbers of scans computed according to the current signal intensity and to save the data in a given format.

All the ST-1000 control and spectrum acquisition procedures have hence been extracted from the original programme source to be afterwards integrated in a larger programme including not only the experiment automation but also the spectra analysis. Both have been developed in C language.

The principle of measurements is based on DOAS method described before. The Sun is the present light source in use. In order to eliminate Fraunhofer absorption lines, the raw spectrum is first divided by a reference spectrum obtained with small zenith angle. After wavelength alignment, the resultant ratio spectrum contains only atmospheric absorption features. After transformation into a differential spectrum, the atmospheric concentration is obtained by fitting the differential optical thickness calculated with the absorption cross-sections of atmospheric molecules obtained from the scientific literature or measured in the laboratory (see Section II.2) with the observed differential optical thickness. An artificial light source will be utilized for long path

measurements in the troposphere.

The experiment automation and spectrum analysis bloc diagrams are presented in figures 13 to 15. The complete automation program has been successfully tested over a period of time of ten days. In addition, some atmospheric observations of NO₂ and ozone have been performed, in Brussels for algorithm development and testing (figures 16 and 17).

IV General Conclusions and Future Works

In the course of 1991 the Belgian groups involved in TOPAS have essentially constructed two instrumental set ups allowing to measure minor constituents of the troposphere in the UV/Visible region. Each instrument is different; one is based on the cheaper more movable grating spectrometer using a diode array detector; the other is a more expensive but more performing Fourier spectrometer which is not movable.

The next steps in the present research are obvious.

1. It is imperative to perform an intercomparison of results with both instruments. For this purpose it is envisaged in the course of 1992 to proceed to simultaneous measurements on the Campus of the Université Libre de Bruxelles. This will imply not only an examination of the hardware advantages of each set up also a crosscheck of the data processing procedures. Spectra obtained with one instrument will be analysed by the algorithms used by the other. It has been suggested that this campaign be extended to other groups in the TOPAS subproject who dispose of a movable instrument. Tentative acceptances from the French, German and Swedish groups have been received (see general report).
2. A second aim which will be undertaken is the automation of the ULB set up. Present measurements require the permanent presence of a scientific personnel for a period of 24 hours. Measurements are thus limited in number and a partial or total automation of the data acquisition is necessary.
3. Finally it is obvious that the non-portability of the Fourier set up is a handicap for future collaboration with other EUROTRAC subprojects. Funding is being requested (and presently partially obtained) in order to acquire a new field Fourier spectrometer (BRUKER IFS120M).

Communications

1. Detection of O₃, NO₂ and SO₂ in an urban atmosphere by differential absorption using Fourier Transform Spectroscopy, A.C. Vandaele, M. Carleer, R. Colin, P.C. Simon, XVI General Assembly of the European Geophysical Society, Wiesbaden, 22-26 April, 1991, *Annales Geophysicae*, suppl. 9, C241-C242, 1991
2. Detection of minor constituents in an urban atmosphere using Fourier Transform Spectroscopy, M. Carleer, R. Colin, A.C. Vandaele, P.C. Simon, XX General Assembly IUGG (session IAMAP), Vienne, 11-24 August, 1991
3. Spectroscopic measurements of atmospheric changes (SMAC), P.C. Simon, L. Delbouille, R. Colin, IGBP-Related Research in Belgium, Royal Belgian Academies of Sciences, Brussels, Oct. 23, 1991

Publications

1. Detection of minor tropospheric constituents using Fourier Transform Spectroscopy, M. Carleer, R. Colin, A.C. Vandaele, P.C. Simon, *Optical Remote Sensing of the Atmosphere*, Williamsburg, Virginia, 18-21 November, 1991, *Technical Digest Series*, vol 18, 278-280, 1991

References

- [1] Stull D., Prophet H., JANAF Thermochemical Tables, 2nd ed., NSRDS-NBS37, June 1971.
- [2] Bass A., Ledfort A., Laufer A., Extinction Coefficients of NO₂ and N₂O₄, J. Research of the NBS, A Physics and Chemistry, Vol 80A, No 2, March-April 1976
- [3] Hall T., Blacet F., J. Chem. Phys., 20, 1745, 1952
- [4] Schneider W., Moortgat G., Tyndall G., Burrows J., Absorption cross sections of NO₂ in the UV and visible region (200-700 nm) at 298 K, J.Photochem. and Photobiol., 40A, 195-217, 1987
- [5] Thomsen O., Messung des Absorptionswirkungsquerschnitts von Schwefeldioxyde in Wellenlängenbereich von 265 bis 298 nm, GKSS-Forschungszentrum, GKSS 90/E/36, 1990
- [6] Daumont D., Barbe A., Brion J., Malicet J., New absolute cross section of O₃ in the 195-350 nm spectral region, personal communication
- [7] Pommereau J.P., Goutail F., Laville P., Development of differential absorption spectroscopy for atmospheric trace species monitoring, Eurotrac Annual Report 1989
- [8] Platt U., Perner D., Direct Measurements of atmospheric CH₂O, HNO₂, O₃ and SO₂ by Differential Optical Absorption in the near UV, J. Geo. Res., 85(C12), 7453-7458, 1980
- [9] Plane J., Nien C., A differential optical absorption spectrometer for measuring atmospheric trace gases, accepted for publication in Review of Scientific Instruments, 1992
- [10] DeMore W.B., Sander S.P., Golden D.M., Molina M.J., Hampson R.F., Kurylo M.J., Howard C.J., Ravishankara A.R., Chemical, kinetics and photochemical data for use in the stratosphere modelling Evaluation No 9, JPL Publication No 90-1, January 1, 1990
- [11] Parrish D.D., Murphy P.C., Albritton D.L., Fehsenfeld F.C., The measurement of the photodissociation rate of NO₂ in the atmosphere, Atmos. Environ., 17, 1365, 1986
- [12] ST-1000 Software Manual, PI, Inc.

Acknowledgments

This project has been supported by the Belgian State - Prime Minister's Service - Science Policy Office and the "Fonds National de la Recherche Scientifique". We would like to also thank D. De Muer (Koninklijke Meteorologische Instituut) and the Institute for Hygiene and Epidemiology for the data they have provided.

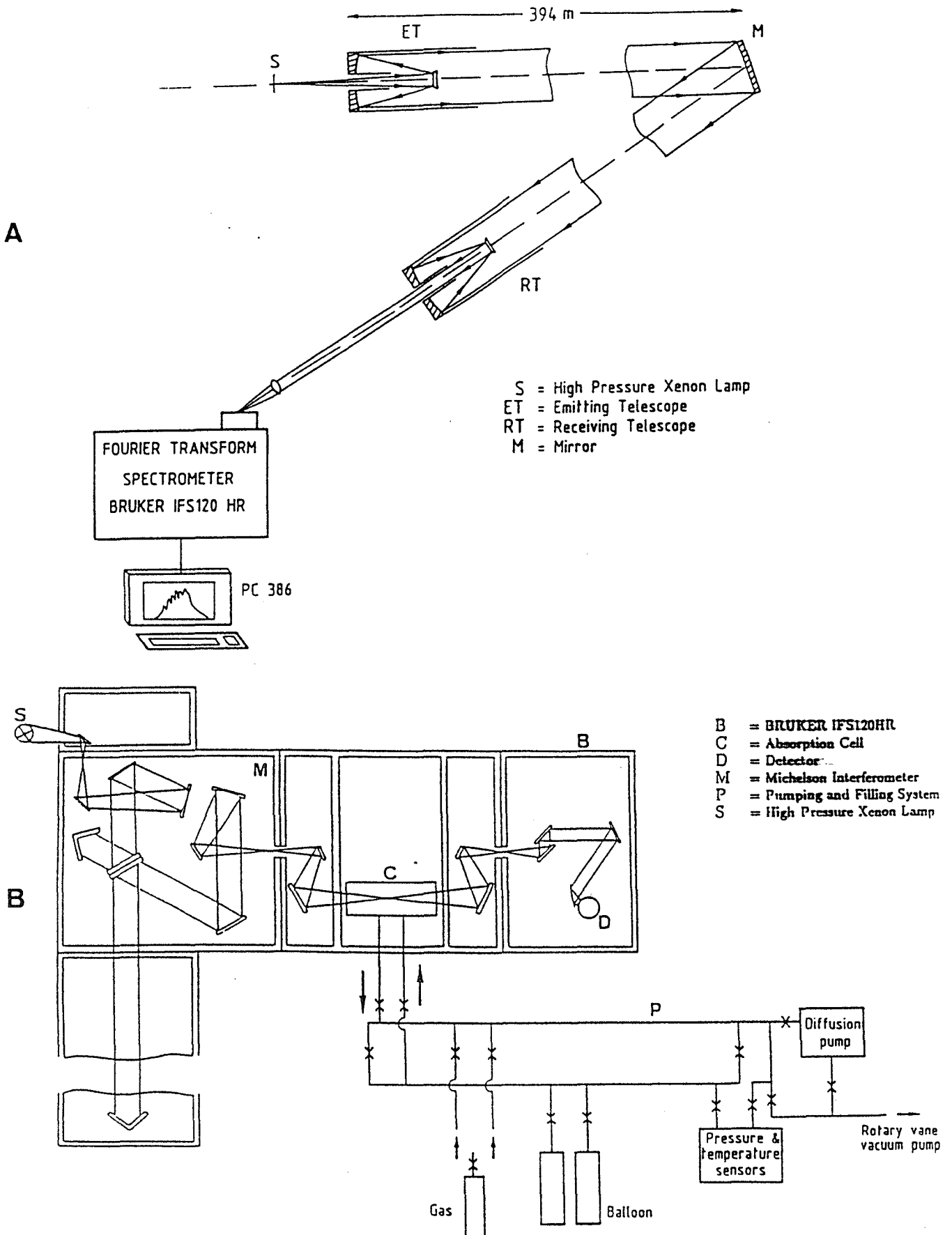


Fig. 1 : Experimental set up

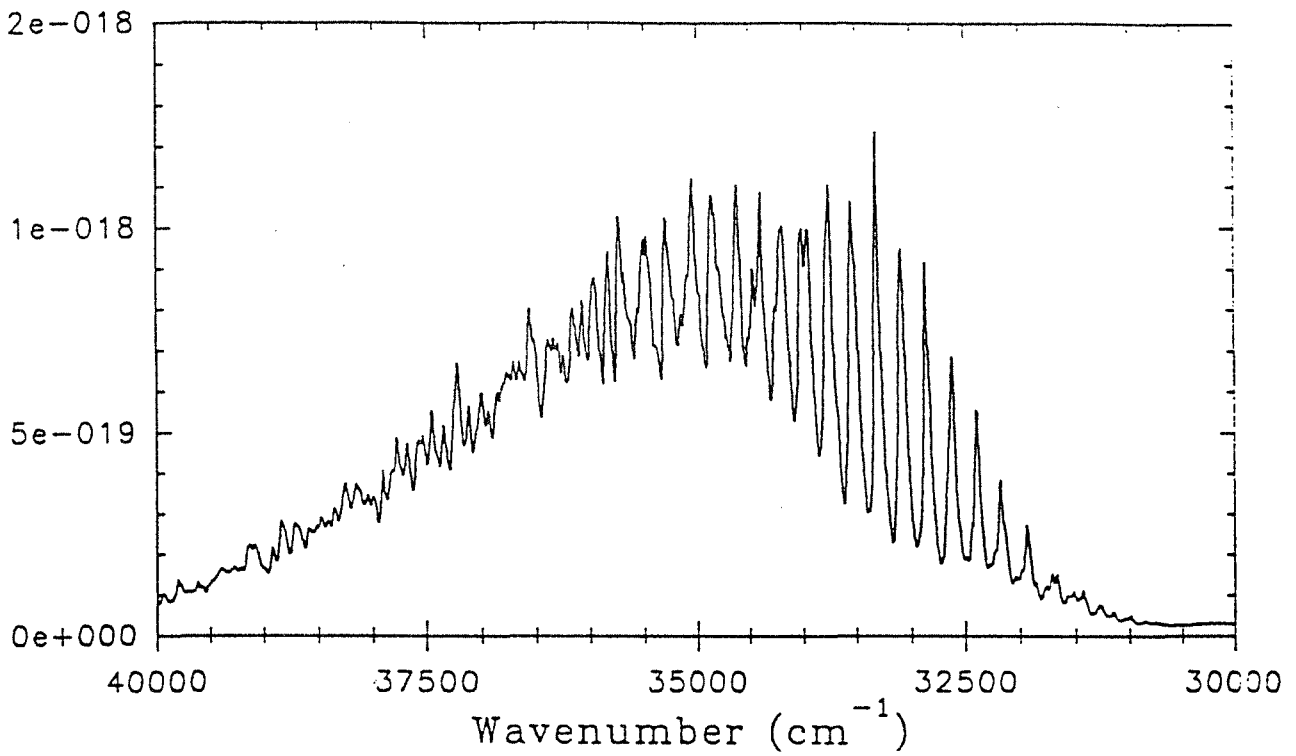


Fig. 2 : Absolute absorption cross section of SO₂ (cm²/molec)

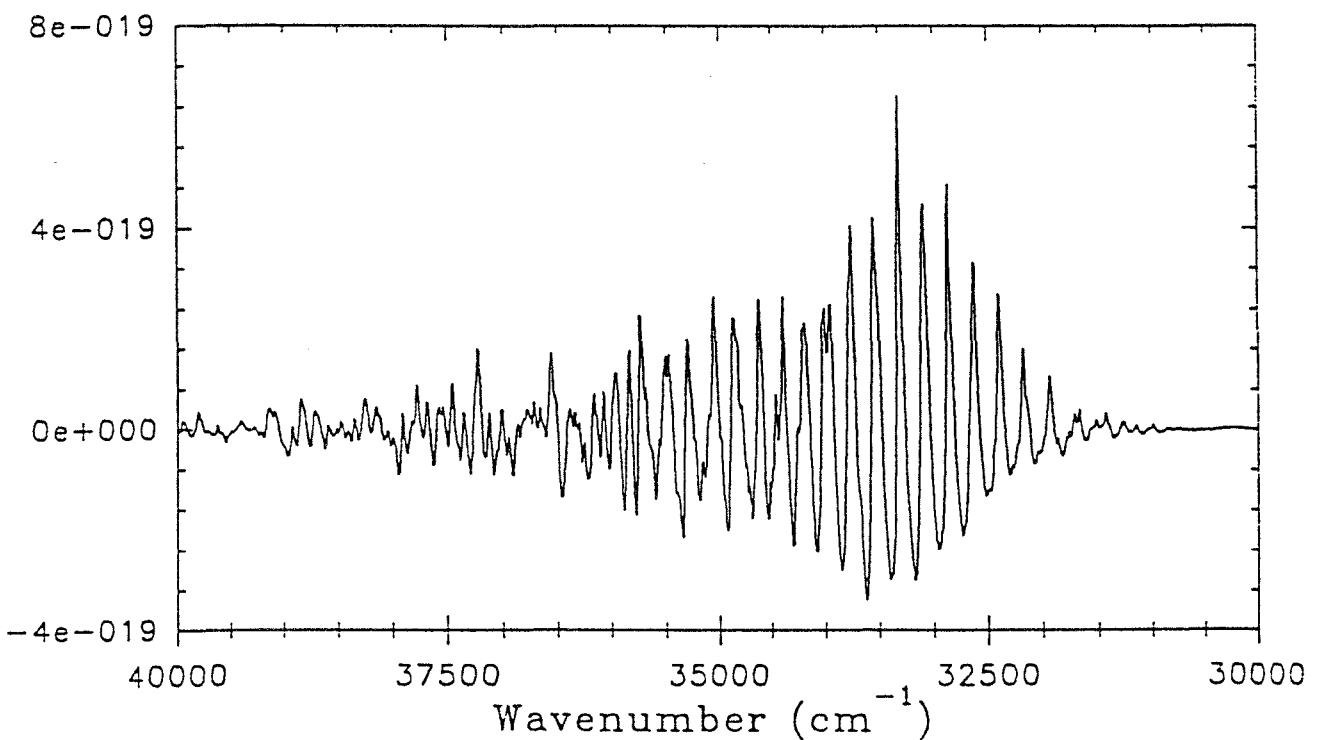


Fig. 4 : Differential absorption cross section of SO₂ (cm²/molec)

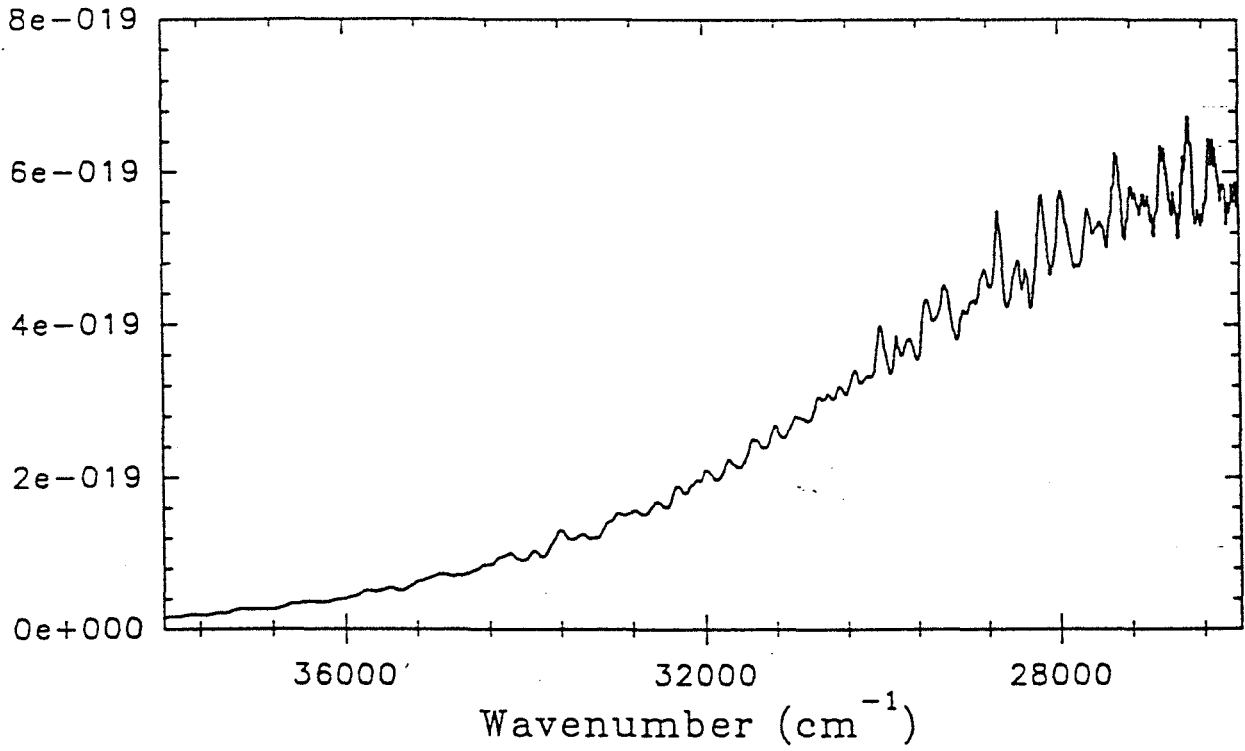


Fig. 3 : Absolute absorption cross section of NO₂ (cm²/molec)

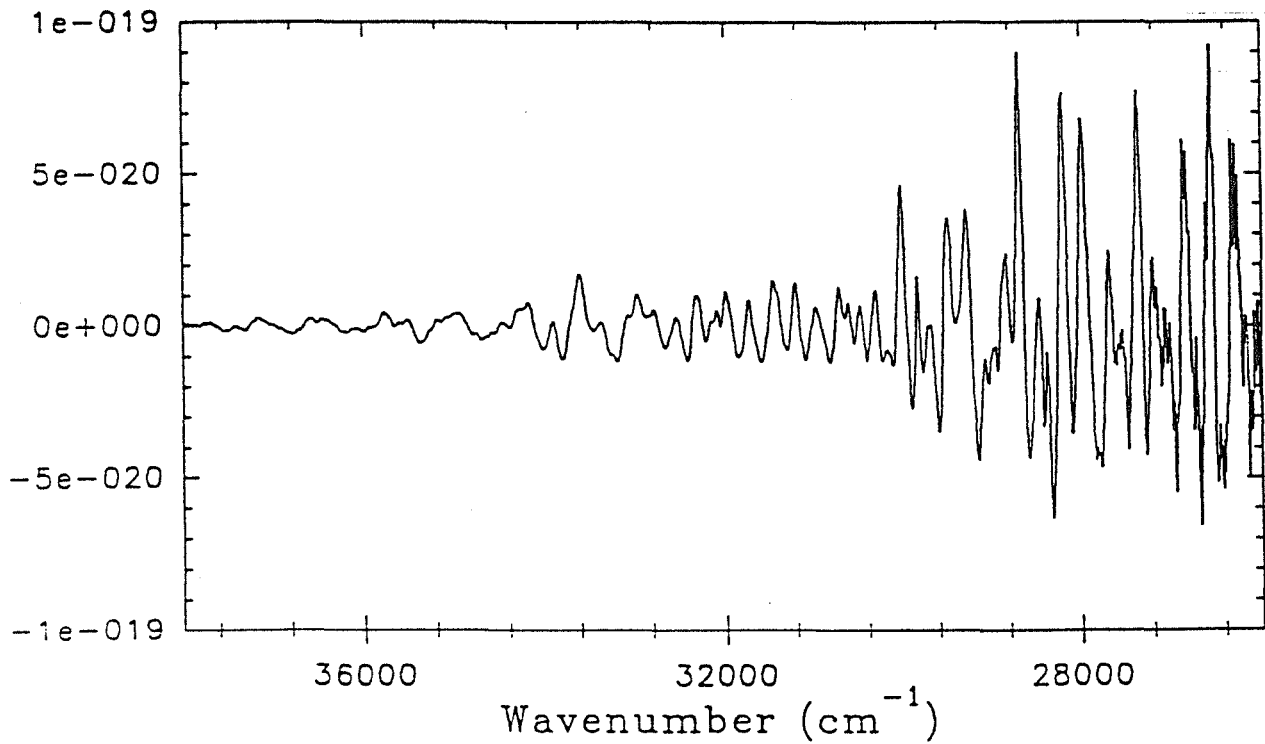


Fig. 5 : Differential absorption cross section of NO₂ (cm²/molec)

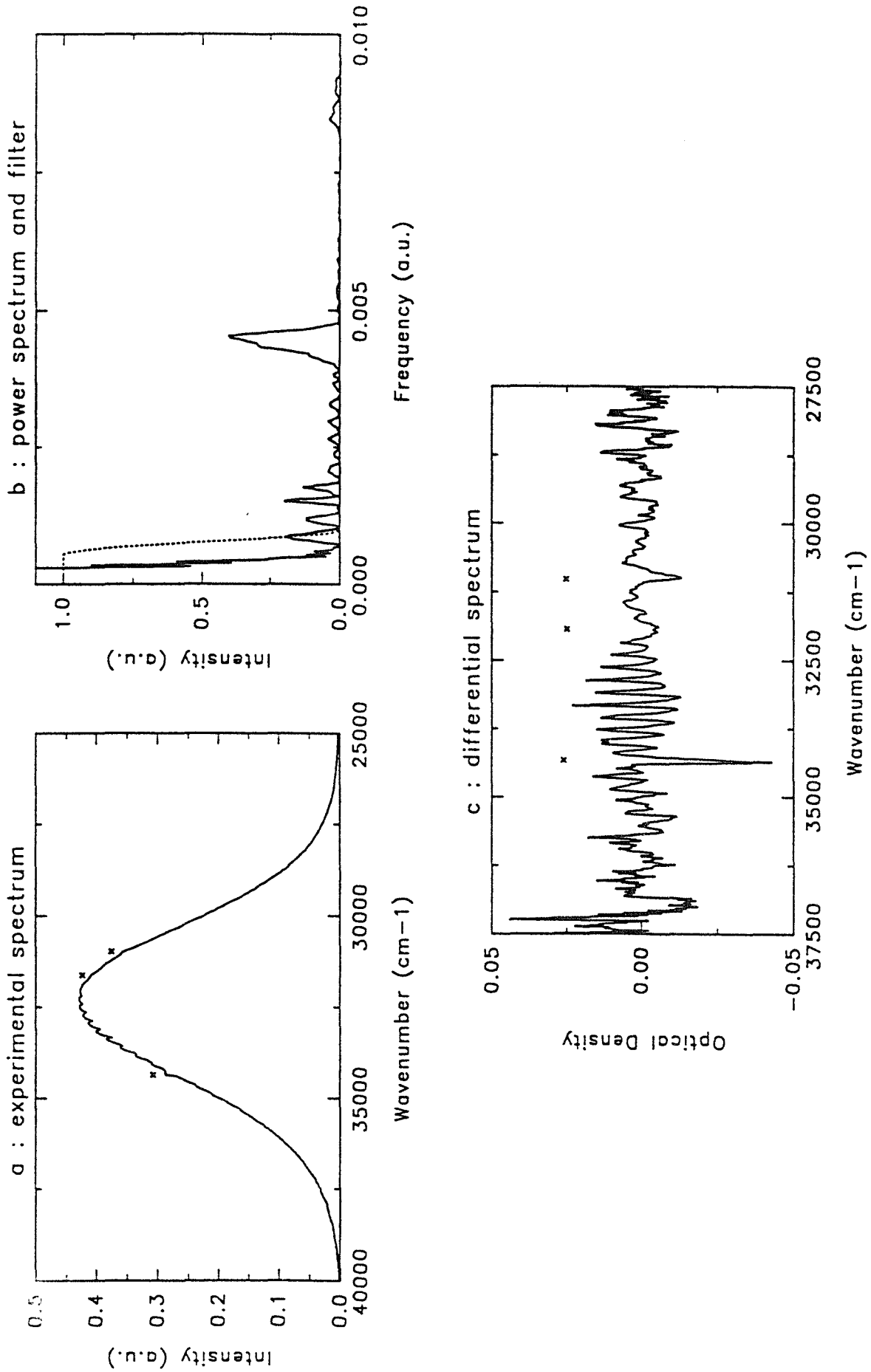


Fig. 6 : Different stages of the analysis (stars show the emission peaks of the Xe lamp)

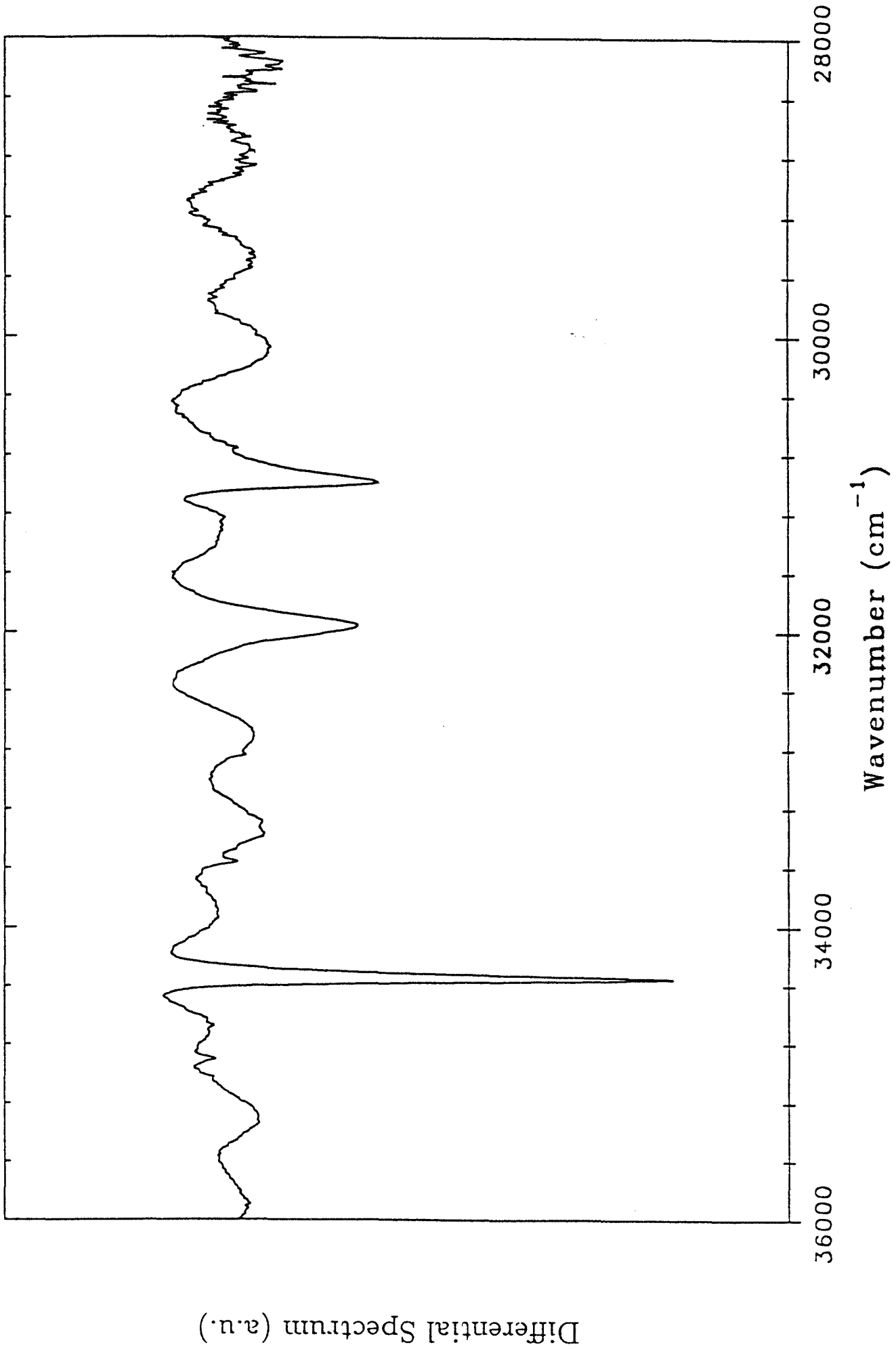


Fig. 7 : Absorption structures of the Xenon lamp

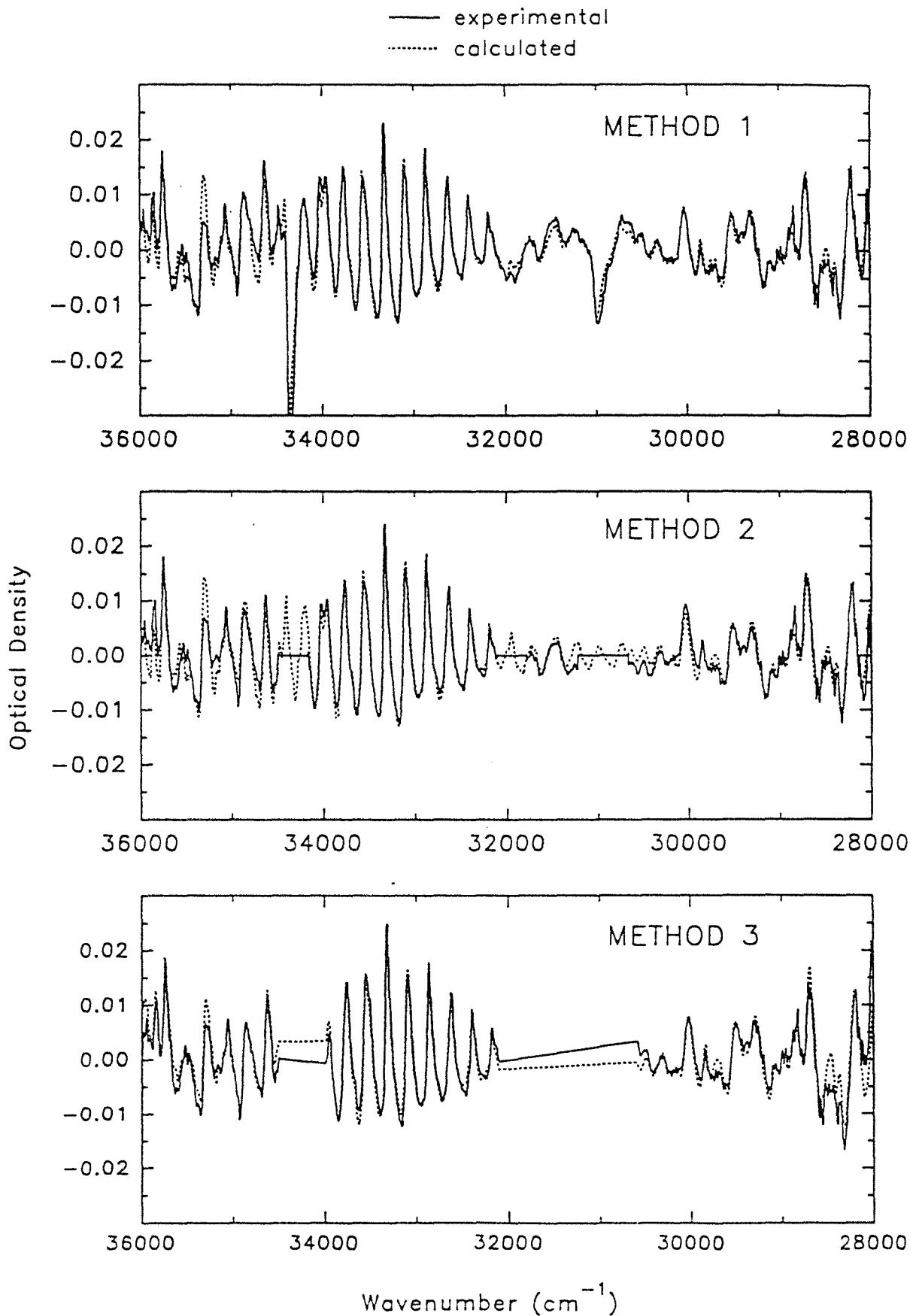


Fig. 8 : Comparison of the three methods

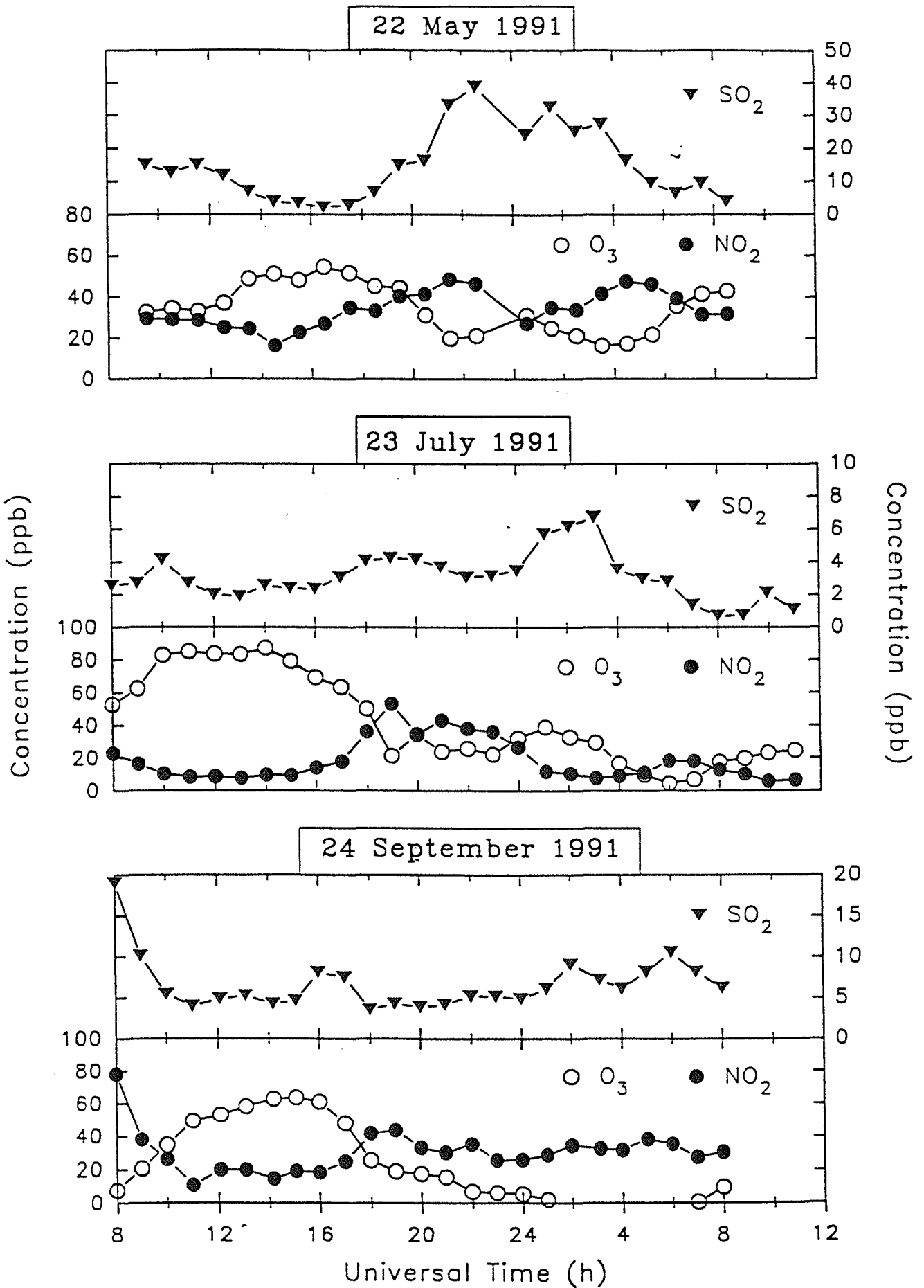
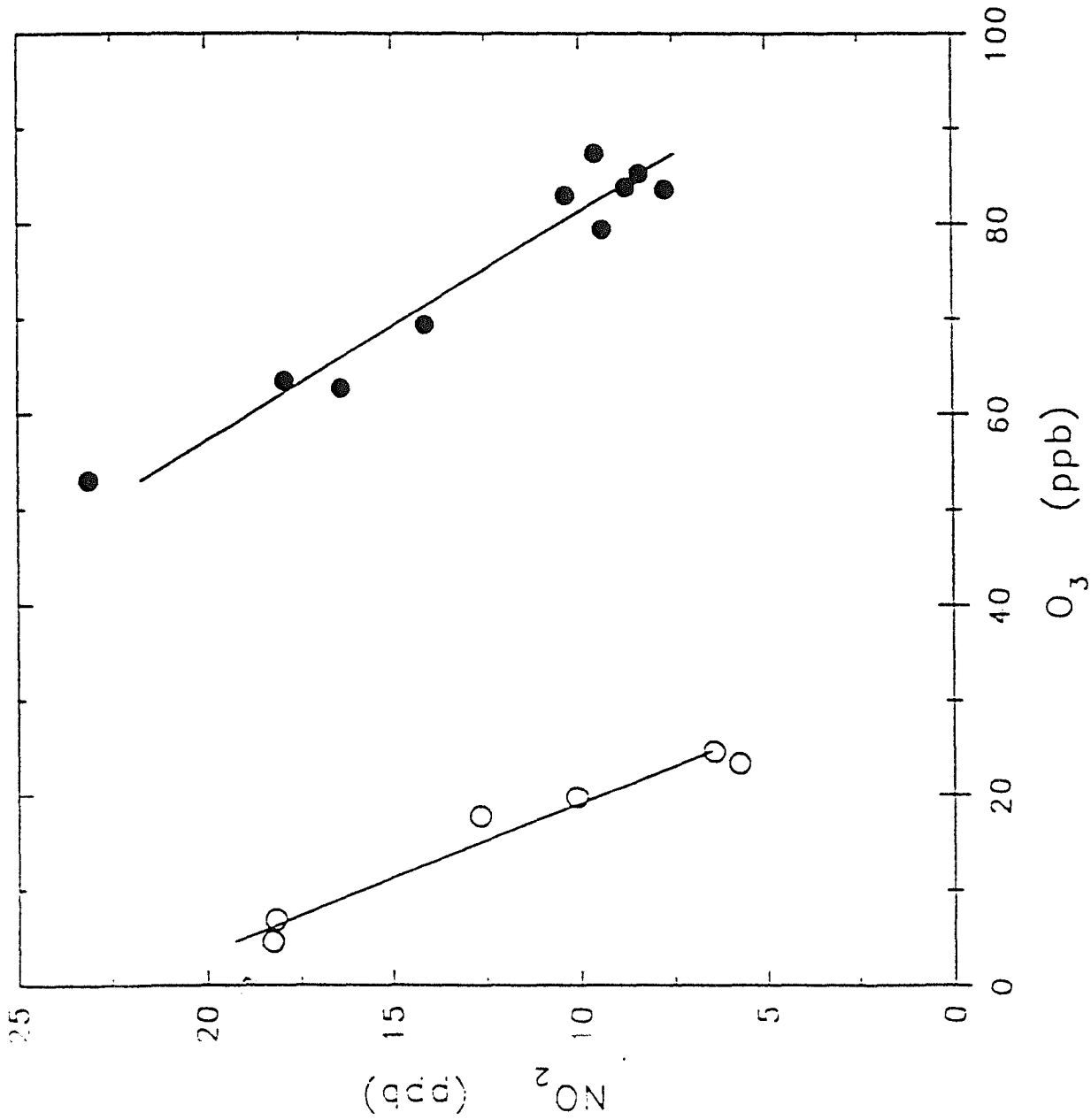


Fig. 9 : Concentration profiles of SO₂, NO₂ and O₃



● : 23/7/91
 $r=0.97$
 st.dev._{NO₂} = 1.3
 st.dev._{O₃} = 3.1

○ : 24/7/91
 $r=0.98$
 st.dev._{NO₂} = 1.3
 st.dev._{O₃} = 2.0

Fig. 10 : Correlation between O₃ and NO₂ day concentrations for the two days May 23 and 24, 1991

19/2/91

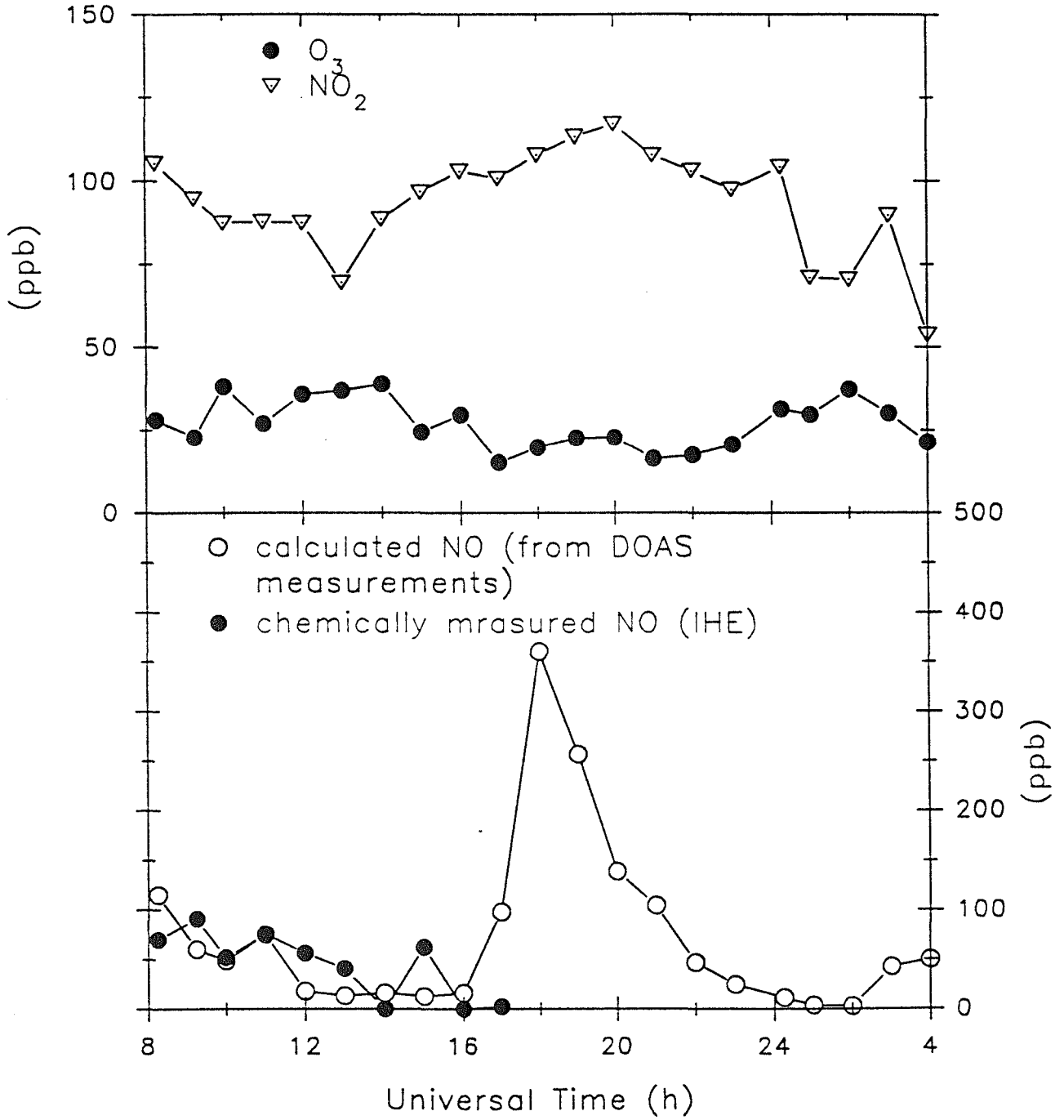


Fig. 11 : NO concentration profile

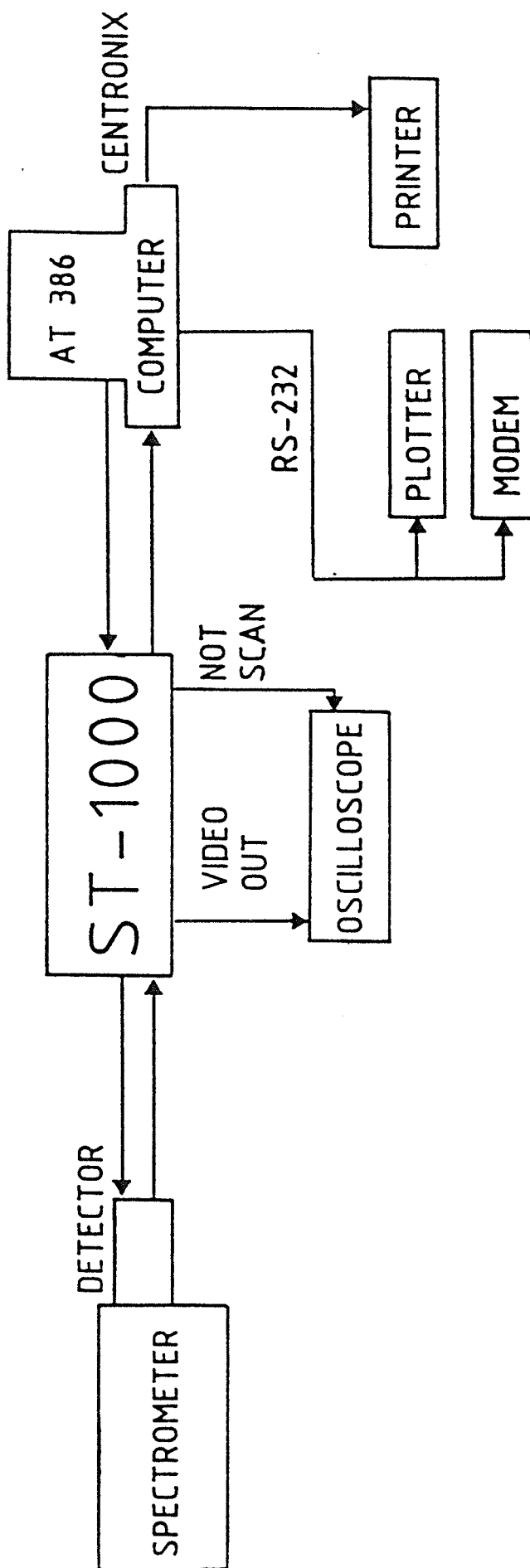


Fig. 12 : Hardware and software interface with the instrument

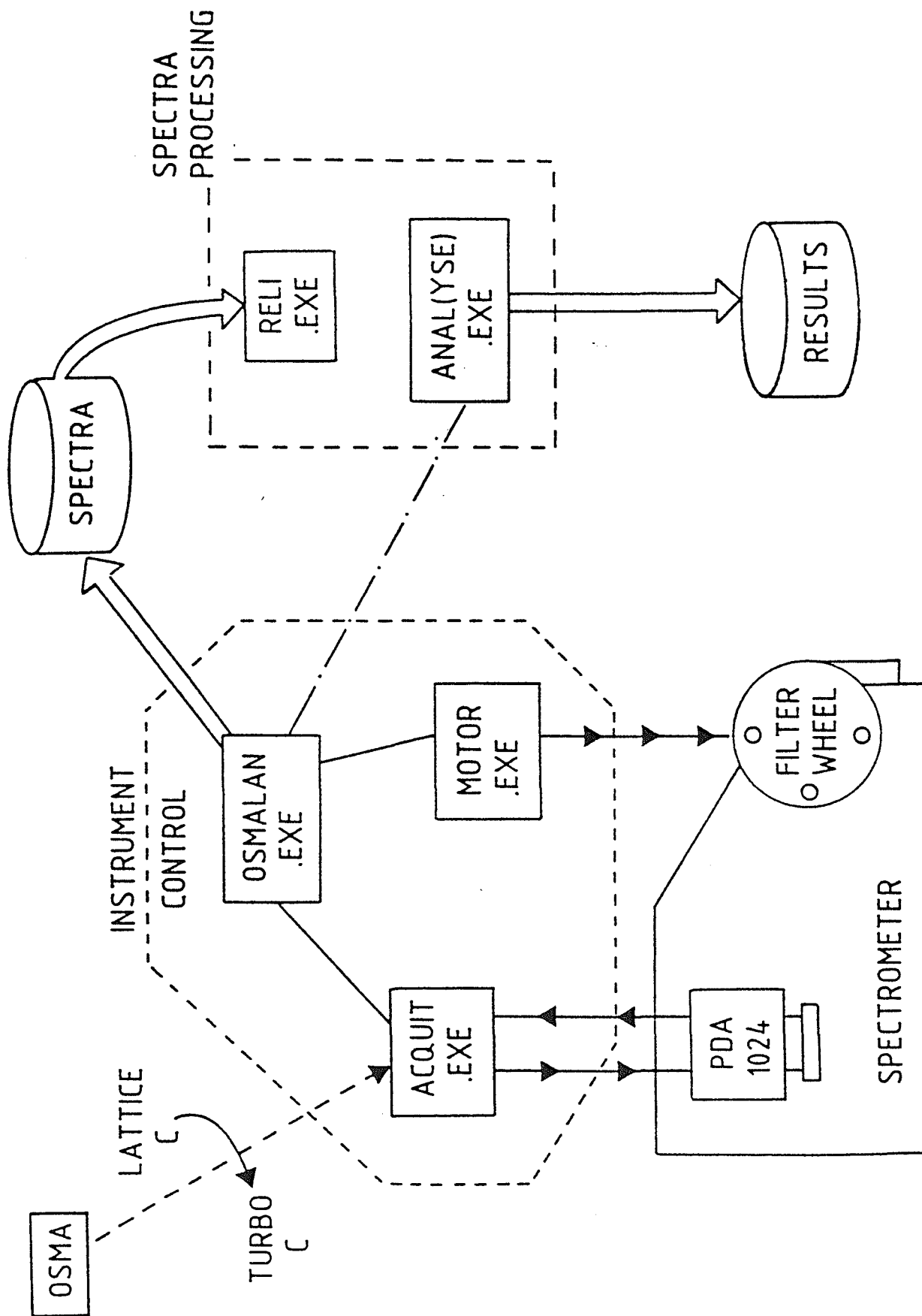


Fig. 13 : Bloc diagram showing the organisation of the programs developed for the automation of a PDA spectrograph

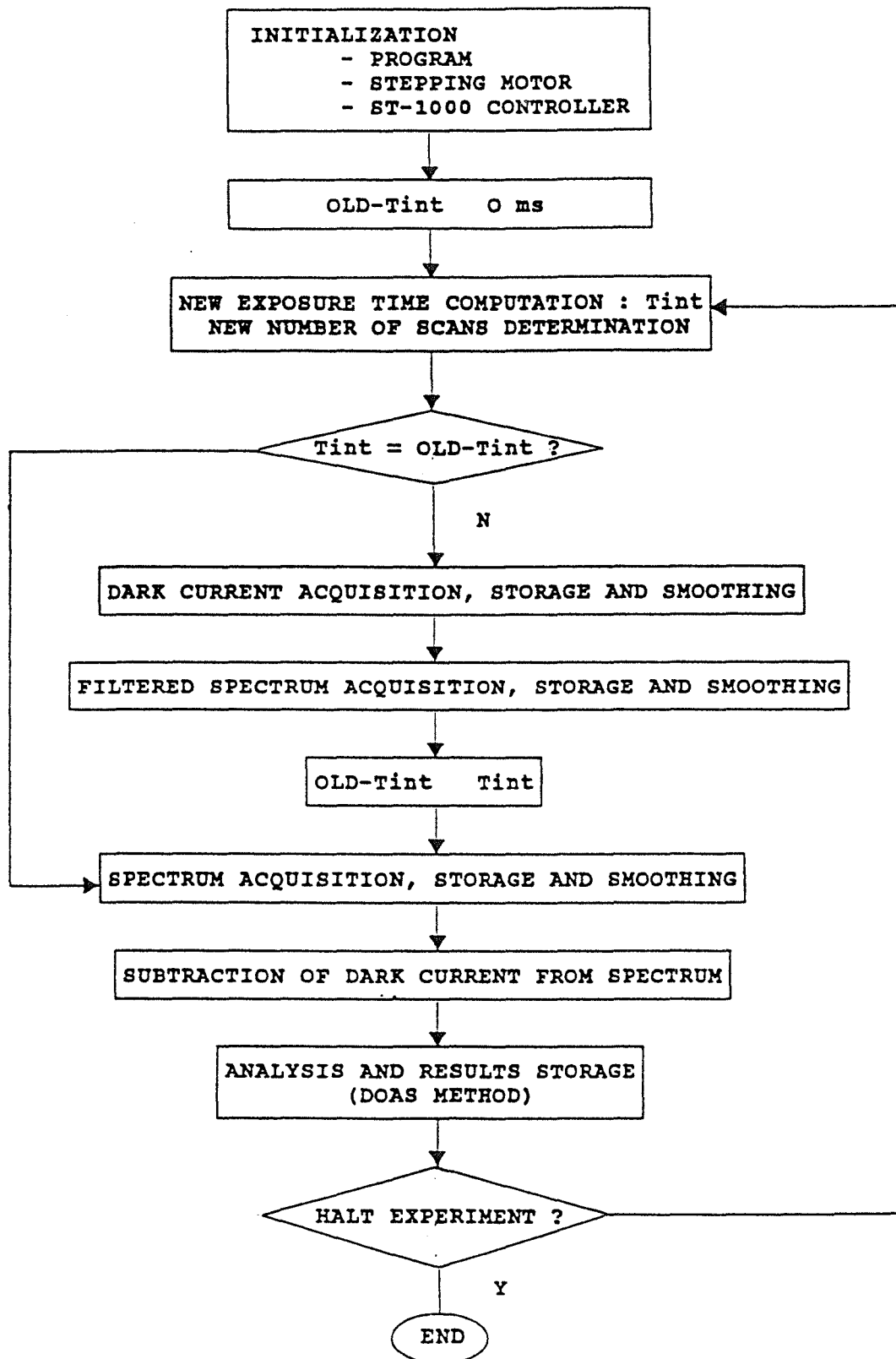


Fig. 14 : Bloc diagram of the experiment control program (OSMALAN.EXE)

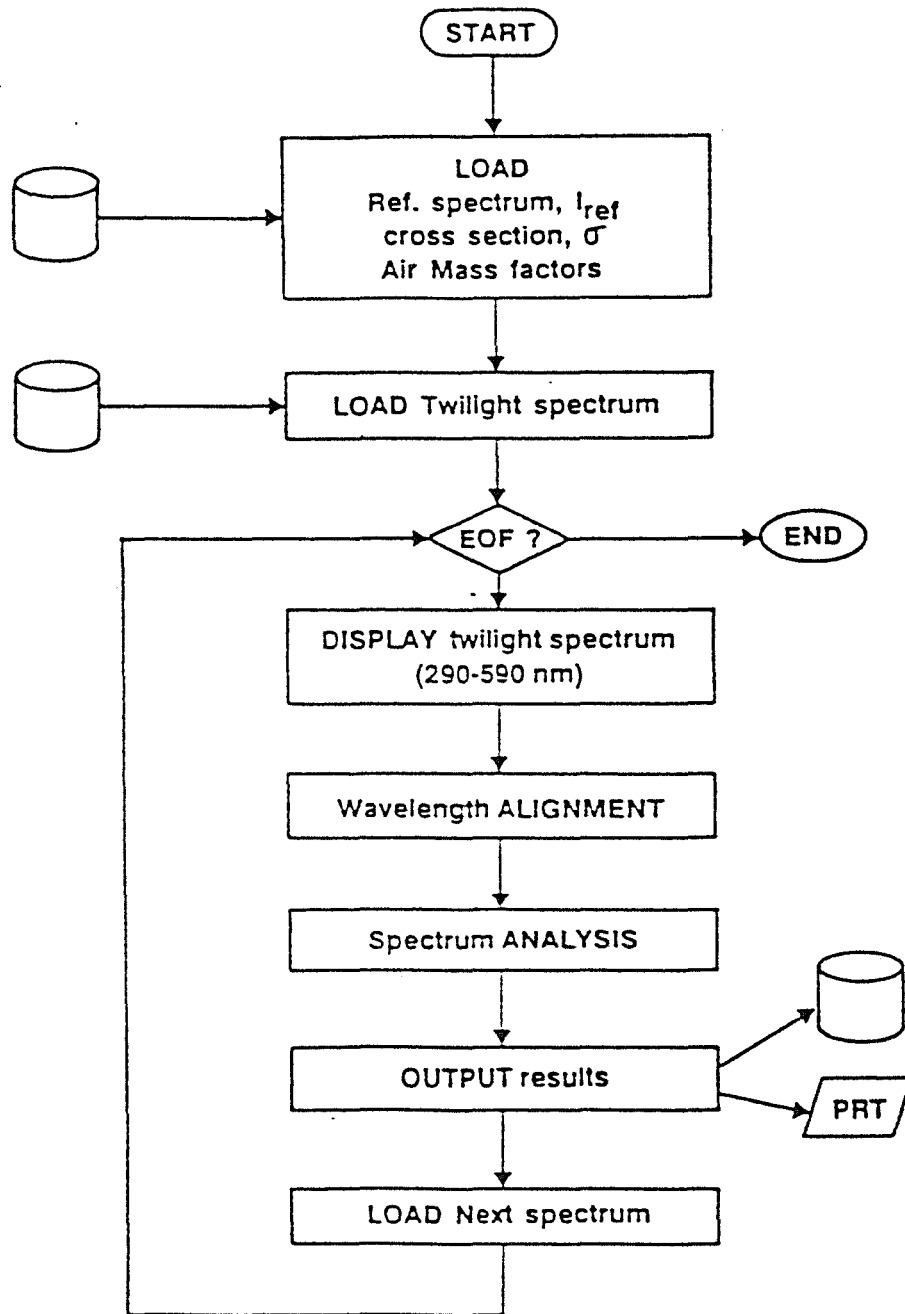


Fig. 15 : Bloc diagram of the spectrum analysis program (ANAL(YSE).EXE)

— experimental optical thickness
... calculated optical thickness

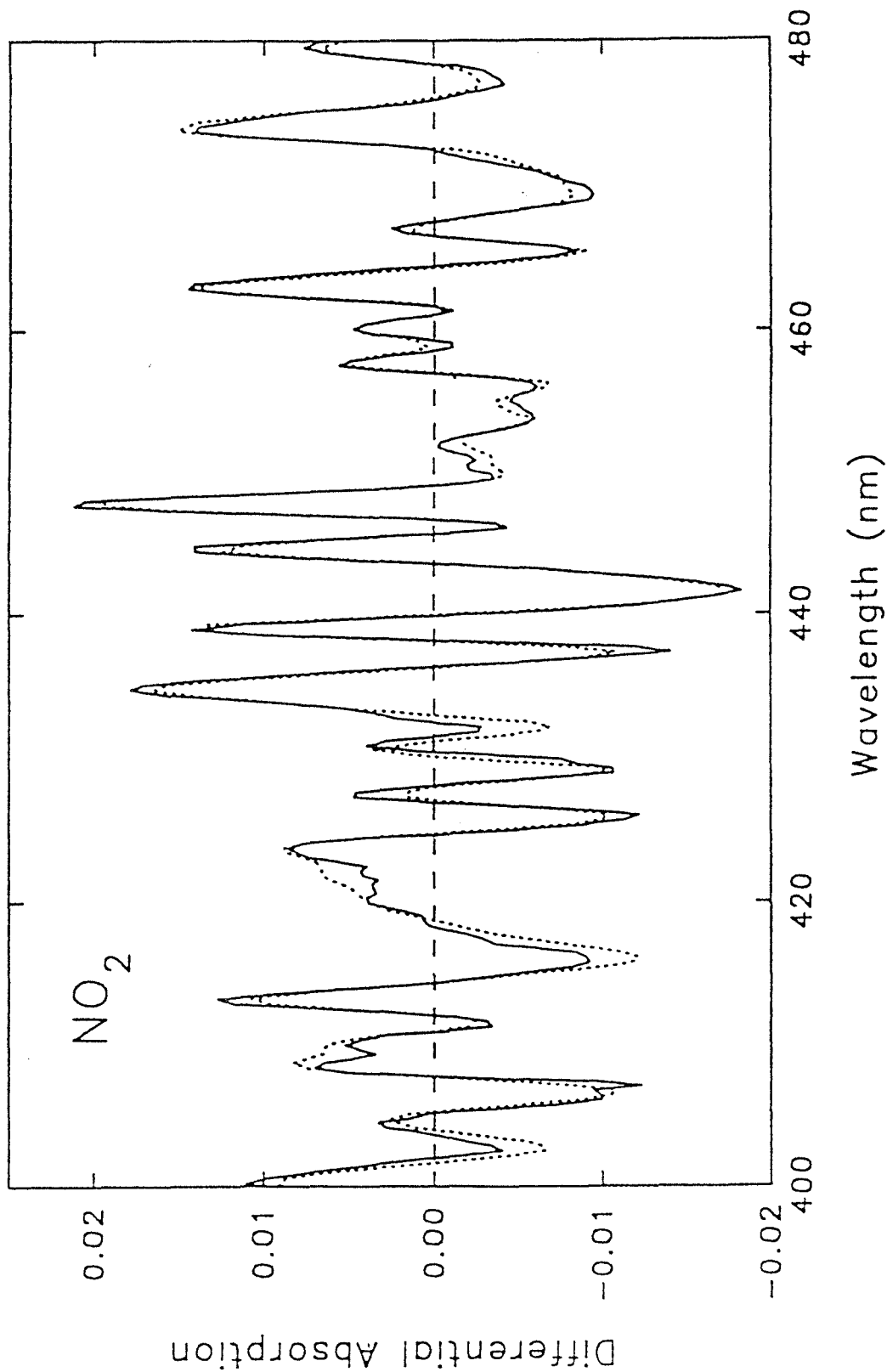


Fig. 16 : Comparison of the experimental (—) and calculated (....) optical thickness in the 400-480 nm spectral region where NO_2 is the main absorber

— experimental optical thickness
... calculated optical thickness

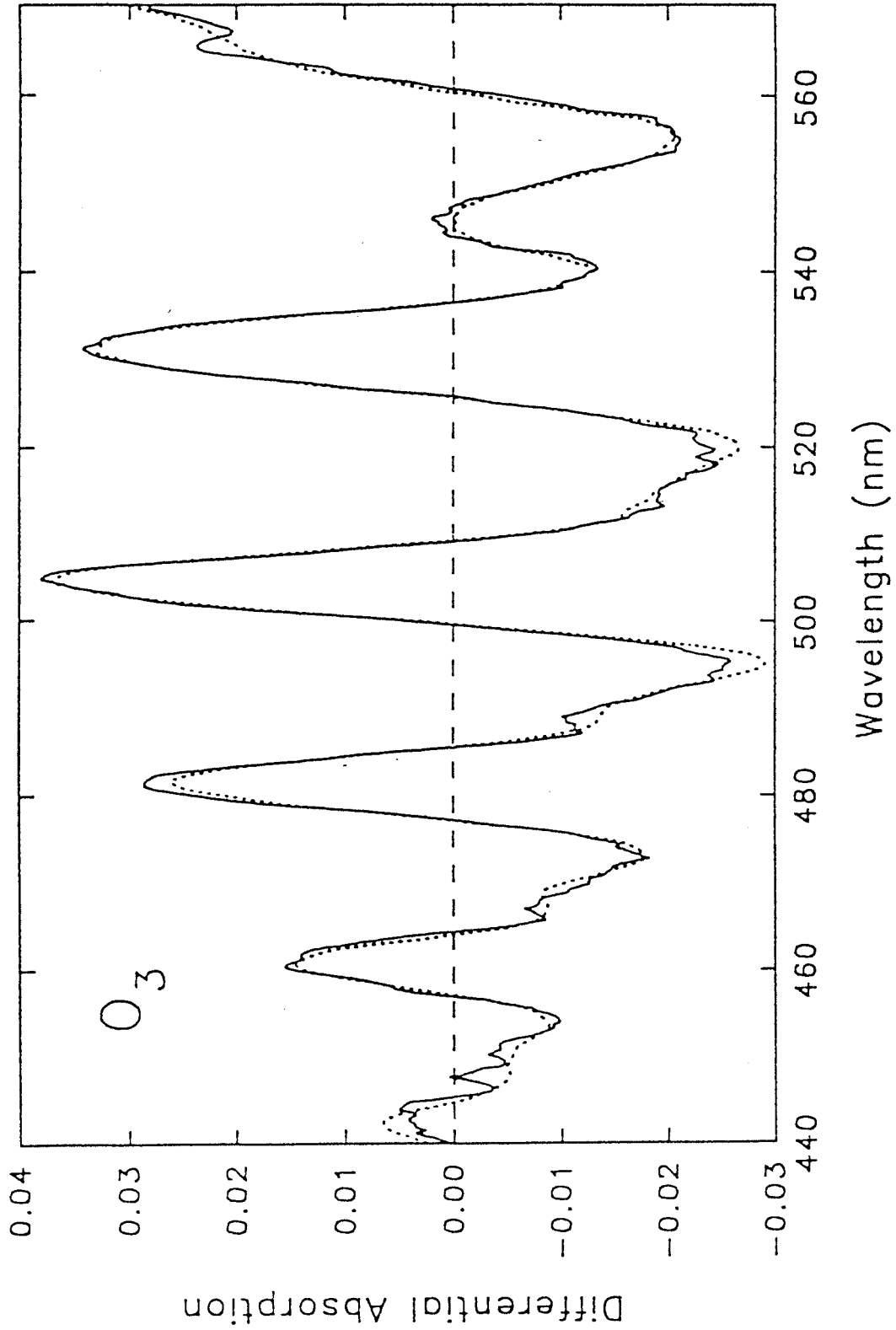


Fig. 17 : Comparison of the experimental (—) and calculated (...) optical thickness in the 440-570 nm spectral region where O_3 is the main absorber

DEVELOPMENT OF A LONG PATH UV-VISIBLE SPECTROMETER FOR ATMOSPHERIC COMPOSITION MONITORING

A contribution to the EUROTRAC subproject TOPAS

J. P. Pommereau, F. Goutail, P. Laville, M. Nunez-Pinharanda
Service d'Aéronomie du CNRS
Verrières le Buisson, 91371 France

Summary

Since 1989, a long path diode array spectrometer using a single telescope for emission and reception and a reflector at the other end, was developed in the laboratory. In 1991, the instrument was tested in the field operating permanently during several months, first in urban polluted air at Paris and later under cleaner atmospheric conditions in the Vosges in the frame of the ACE-NUAC project. In both cases, performances and uncertainties for each measured constituent were analyzed as well as comparisons with other observations when available. Results show that the precision is now satisfactory but that some more work is needed for improving the absolute calibration for several constituents. The long term testing in automatic mode have also demonstrated several minor defaults which must be corrected before being able to perform totally unattended for months. After modifications and testing, the instrument will participate to the TOPAS intercomparison campaign anticipated for 1992.

Aims of Research

The objective of the subproject is the development of an almost unattended and sensitive instrument for monitoring the composition of the atmosphere by measuring simultaneously several photochemically active constituents absorbing by definition in the uv-visible spectral range. The final objective at the end of the development phase is to make available the instrument for field studies, by industrialization under licensing.

Activities During the Year

In 1991, the objective was the testing and qualification of the instrument. Activities have been conducted into 3 directions: a) measurements and comparisons in urban air conditions (October - February 1991); b) clean atmosphere testing and contribution to ACE - NUAC (April - July 1991); c) Laboratory testing, absolute calibrations and improvement of absorption cross-sections of relevant species (October 1991 -).

Principal Experimental Results

Urban air testing: Measurements were conducted in the center of Paris in collaboration with the local Air Pollution Monitoring association (AIRPARIF), along a 1600 m optical path during 3 months, modified later for a shorter path (1000 m) for measuring uv absorbing gases. The analysis of uncertainties have shown that the two parameters driving the quality of the measurements are: a) atmospheric transmission and quality of the optics which control the precision inversely proportional to the flux and not its root square (figure 1) and b) the quality of the absorption cross-sections introduced in the calculation and their temperature dependences. Average precisions achieved were respectively $0.5 \mu\text{g}/\text{m}^3$ for NO_2 , $0.3 \mu\text{g}/\text{m}^3$ for SO_2 , $6 \mu\text{g}/\text{m}^3$ for O_3 , $0.2 \mu\text{g}/\text{m}^3$ for HNO_2 , $3 \mu\text{g}/\text{m}^3$ for CH_2O and $6 \mu\text{g}/\text{m}^3$ for toluene. Concentrations were found in agreement in average with available in-situ sampling of NO_2 , SO_2 , O_3 and toluene. Direct comparisons with the commercially available DOAS OPSIS show a broad agreement but some significant differences of calibration of the order of 30% for NO_2 and SO_2 ; a total incompatibility (factor 5) of the calibrations of the 2 instruments for CH_2O although it is obvious that they are measuring the same constituent; almost no correlation for ozone and toluene. The analysis of the results of the above test campaign was the subject of the Thesis of P. Laville defended at the University of Paris in February 1992.

Clean atmosphere testing: The objective of the ACE - NUAC is the study of photochemical transformations of air inside clouds. The concept is to measure the air composition with ground instruments below its ascent into a mountain impact cloud, above the cloud with an aircraft and to collect and analyze rainfall water. The campaign which involved several type of instruments and laboratories, was conducted by Météo-France. It has been held in April - June 1991 in the Vosges mountains. Our instrument was part of the ground-based equipment and expected to measure O₃, NO₂, SO₂ and CH₂O. The length of the optical path was 2150 m. Figure 2 shows the results obtained during the 70 days campaign which can be divided into two periods: before day 150 (June 1) where the weather was mostly anticyclonic and therefore during which almost no impact clouds episodes occurred and after this date where an average persistent perturbed flux from the West was recorded with many impact clouds episodes. Figure 2 shows the average difference of air composition between the 2 periods. Wet and rainy conditions are making obviously pollution to be reduced. The following table gives a summary of the results expressed in $\mu\text{g}/\text{m}^3$.

Constituent	Average Conc.	Stand. Dev	1st phase	2nd phase	RMS error
Ozone	68.2	16.7	80	60	6.9
NO ₂	2.9	2.2	5	1.8	0.6
SO ₂	3.6	3.9	6	2	0.5
CH ₂ O	2.3	1.6	3	2	1.8

Preliminary results of the above campaign have been analyzed by A. Salhi in the frame of his Diploma at the University of Paris in September 1991. The detailed analysis in terms of diurnal variations and relations with clouds and precipitations is presently conducted in cooperation with CNRM Météo-France.

Laboratory testing: Besides RMS uncertainties which are principally controlled by light fluxes conditions, the above test campaigns have demonstrated the need for investigating the absolute calibrations of the instrument for the various measured species. A laboratory test programme has started in October 1991 at the industrial laboratory of CERCHAR. Measurements are made in a 2 m long cell filled in sequentially with the various constituents, while the temperature of the room into which the instrument and the cell are placed, can be varied from -40°C to $+40^{\circ}\text{C}$. Although partial results only are available, the following preliminary conclusions can be drawn: a) as far as the optical thickness is lower than about 2, the response of the instrument is linear for the various constituents within the limits of precision; b) although there is a good coherence between optical and in-situ traditional laboratory measurements for NO₂, SO₂, O₃, CH₂O and toluene, differences as large as 30% can be found in absolute calibrations depending on the constituent and the cross-sections used; c) large temperature variations of the calibrations are sometimes present depending on the constituent. This is particularly true for SO₂ which is known to have a large temperature dependence of its absorption cross-sections but poorly known at the moment. Laboratory tests which will be further extended to the study of interferences between gases, are expected to be completed in April 1992.

Main Conclusions

The long path uv-visible spectrometer which was developed at Service d'Aéronomie was thoroughly tested in the field and in the laboratory in 1991. They resulted in a better characterization of the instrument in term of precision, accuracy and long term stability. Although satisfactory in average and of use for field scientific investigations, results have demonstrated some defaults or limitations. Step by step, improvements have been added to the original hard and softwares in order to make the instrument more reliable. A qualification test at an industrial laboratory is presently being conducted. A licence agreement was signed in 1991 with the company Atmos-Equipement which is anticipated to deliver first copies of the developed instrument in April 1992.

Aims of the Coming Year

The main objectives of the following year are to refine the instrument by improving its ability for performing totally unattended, to evaluate its performances by comparison to other developments and new available commercial analyzers and finally increase the number of measured species by

extending the wavelength range toward the uv. Improvements are conducted in the laboratory in cooperation with the industry and comparisons will be performed within the frame of TOPAS at Bruxelles in September 1992.

Acknowledgments

The work was supported by the Ministère de l'Environnement and the Ministère de la Recherche Scientifique et Technique and the collaboration of the Agence de la Qualité de l'Air, which are gratefully acknowledged.

References

1. P. Laville, PHD Thesis, University of Paris VII, February 1992.
2. A. Salhi, Diplome d'Etudes Approfondies, University of Paris VI, September 1991.

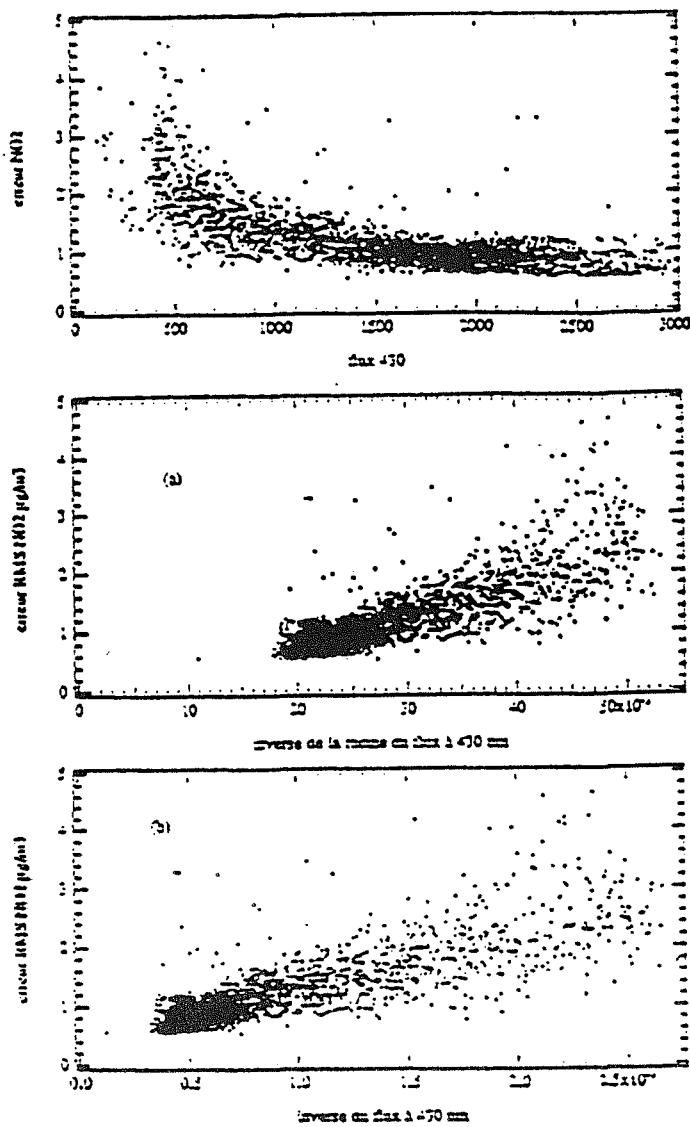


Figure 1. Analysis of error of measurements performed during 3 months at the center of Paris in 1991. Plot a) shows the relation between RMS error issued from the least squares correlation between observed attenuation and absorption cross-sections of the constituent measured in the laboratory and fluxes received from the Xenon lamp. The error increases rapidly when the light falls down, that is when the atmospheric transmission degrades. The length of the optical path must be optimized in order to get the best compromise between sensitivity and RMS error under average weather conditions. The RMS error is plotted vs the inverse of the square root of the flux in plot b) and the inverse of the flux in plot c). The better agreement of the last one shows that the limit of the present system is not the noise of the detector but the limits of the 12 bits AD converter. Similar careful analysis have been conducted for each species, for identifying the limits of each measurement, in order to improve the performances of the instrument.

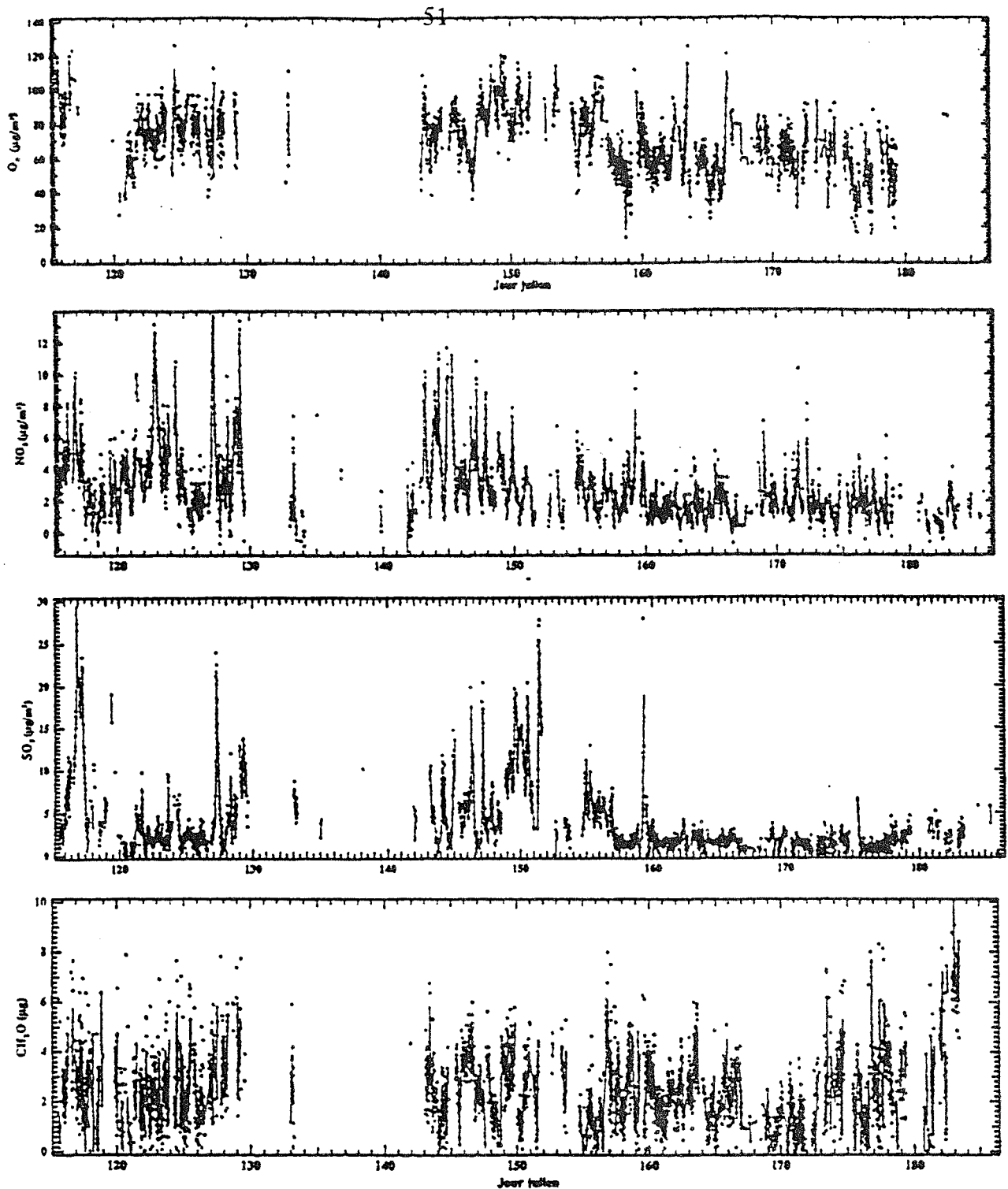


Figure 2. Results of measurements of ozone, NO₂, SO₂ and CH₂O performed during 70 days in the Vosges in Spring 1991 in the frame of the ACE-NUAC project. At the exception of 10 days during which the instrument was stopped, measurements were performed automatically. Most of the peaks are due to diurnal variations. The average difference of concentrations between the first and the second half of the campaign corresponds to different weather conditions. In April and May (before day 150) the weather was anticyclonic, while during the second half, perturbations from the West and rain were frequent and therefore air pollution was reduced.